Biogeosciences Discuss., 11, 14551–14585, 2014
www.biogeosciences-discuss.net/11/14551/2014/
doi:10.5194/bgd-11-14551-2014

Biogeosciences Discussions
Open Access

The mechanisms of North Atlantic CO_2 uptake in a large Earth System Model ensemble

P. R. Halloran[1], B. B. B. Booth[2], C. D. Jones[2], F. H. Lambert[3], D. J. McNeall[2], I. J. Totterdell[2], and C. Völker[4]

[1]Geography, College of Life and Environmental Sciences, University of Exeter, Amory Building, Rennes Drive, Exeter, EX4 4RJ, UK
[2]Met Office Hadley Centre, FitzRoy Road, Exeter, Devon, EX1 3PB, UK
[3]Exeter Climate Systems, College of Engineering, Mathematics and Physical Sciences, University of Exeter, Harrison Building, North Park Road, Exeter, EX4 4QF, UK
[4]Alfred Wegener Institute Helmholz Center for Polar and Marine Research, Alfred Wegener Institute, Am Handelshafen 12, 27570 Bremerhaven, Germany

Received: 15 September 2014 – Accepted: 25 September 2014 – Published: 13 October 2014

Correspondence to: P. R. Halloran (p.halloran@exeter.ac.uk)

Published by Copernicus Publications on behalf of the European Geosciences Union.

Abstract

The oceans currently take up around a quarter of the carbon dioxide (CO_2) emitted by human activity. While stored in the ocean, this CO_2 is not influencing Earth's radiation budget; the ocean CO_2 sink therefore plays an important role in mitigating global warming. CO_2 uptake by the oceans is heterogeneous, with the subpolar North Atlantic being the strongest CO_2 sink region. Observations over the last two decades have indicated that CO_2 uptake by the subpolar North Atlantic sink can vary rapidly. Given the importance of this sink and its apparent variability, it is critical that we understand the mechanisms behind its operation. Here we explore subpolar North Atlantic CO_2 uptake across a large ensemble of Earth System Model simulations, and find that models show a peak in sink strength around the middle of the century after which CO_2 uptake begins to decline. We identify different drivers of change on interannual and multidecadal timescales. Short-term variability appears to be driven by fluctuations in regional seawater temperature and alkalinity, whereas the longer-term evolution throughout the coming century is largely occurring through a counterintuitive response to rising atmospheric CO_2 concentrations. At high atmospheric CO_2 concentrations the contrasting Ravelle factors between the subtropical and subpolar gyres, combined with the transport of surface waters from the subtropical to subpolar gyre, means that the subpolar CO_2 uptake capacity is largely satisfied from its southern boundary rather than through air–sea CO_2 flux. Our findings indicate that: (i) we can explain the mechanisms of subpolar North Atlantic CO_2 uptake variability across a broad range of Earth System Models, (ii) a focus on understanding the mechanisms behind contemporary variability may not directly tell us about how the sink will change in the future, (iii) to identify long-term change in the North Atlantic CO_2 sink we should focus observational resources on monitoring subtropical as well as the subpolar seawater CO_2, (iv) recent observations of a weakening subpolar North Atlantic CO_2 sink suggests that the sink strength is already in long-term decline.

BGD
11, 14551–14585, 2014

1 Introduction

Our limited understanding of how the CO_2 emission to atmospheric CO_2 (CO_2^{atm}) concentration ratio will evolve through time constitutes one of the largest components of uncertainty in future climate projections (Booth et al., 2012). To constrain how this airborne fraction of CO_2 might change, and thereby link physical climate understanding to the development of CO_2 emission policy, we need to understand the behaviour of the major terrestrial and marine CO_2 sources and sinks (Friedlingstein et al., 2006).

Earth System Models (ESMs) are the most advanced tools we have available to calculate the link between CO_2 emissions and CO_2 concentrations. At a globally-averaged scale, the current generation of Earth System Models, those developed and run for CMIP5 (Taylor et al., 2012), the 5th Climate Model Intercomparison Project, show good agreement on 21st Century global ocean CO_2 uptake. With the exception of INM-CM4.0 (Volodin et al., 2010) the CMIP5 inter-model globally averaged ocean CO_2 uptake differences are smaller than the inter-scenario differences (Jones et al., 2013). At a regional level however, models do not agree. Furthermore, regional CO_2 uptake can behave very differently from that of the global mean (Fig. 2).

We need to understand the mechanisms behind differences in regional uptake to help us (i) validate models, and (ii) identify where and how to focus observations.

Whilst the carbon-cycle community is developing an increasingly comprehensive understanding of the mechanisms behind recent ocean CO_2 uptake variability in the North Atlantic (e.g. McKinley et al., 2004, 2011; Thomas et al., 2008; Ullman et al., 2009; Metzl et al., 2010; Perez et al., 2013; Schuster and Watson, 2007), the Southern Ocean (e.g. Lenton and Matear, 2007; Le Quere et al., 2007; Lovenduski et al., 2013; Sallee et al., 2012; Ito et al., 2010; Lenton et al., 2009; Verdy et al., 2007), and potential broad-scale future ocean CO_2 uptake changes (e.g. Marinov et al., 2008; Murnane et al., 1999; Roy et al., 2011; Sarmiento and LeQuere, 1996), our understanding of the specific future mechanisms of change projected within comprehensive ESMs in these regions is much more limited (Seferian et al., 2012; Russell et al., 2006; Halloran,

BGD
11, 14551–14585, 2014

2012). Here we attempt to develop our understanding of the possible mechanisms controlling future subpolar North Atlantic CO_2 uptake within Earth System Models.

To understand why the North Atlantic CO_2 sink may be vulnerable to change, it is useful to review the factors that make the region such an intense CO_2 sink (McKinley et al., 2011; Watson et al., 2009; Schuster et al., 2013). Present-day high CO_2 uptake in the subpolar North Atlantic occurs because water that moves northwards as part of the Atlantic Meridional Overturning Circulation (AMOC) experiences steep thermal and chemical gradients and high biological activity (Rayner et al., 2003; Key et al., 2004; Carr et al., 2006). Biological activity exports carbon to depth in the form of sinking biological material, reducing surface carbon concentrations and increasing the air–sea CO_2 gradient. The cooling of water increases the solubility of CO_2 and speciates carbon into forms other than CO_2 (e.g. Zeebe and Wolf-Gladrow, 2001), further increasing the air–sea CO_2 gradient. Deep convection then removes water from contact with the atmosphere, potentially before it has had time to come into air–sea CO_2 equilibrium, maintaining a continuous strong air–sea CO_2 gradient – and therefore flux (Takahashi et al., 2009). A further complicating factor in the North Atlantic is that limited mixing between the subtropical and subpolar gyres allows the development of a strong biogeochemical gradient between waters with a high alkalinity to dissolved-carbon ratio (the warm and saline low-latitude waters), and waters with a low alkalinity to dissolved-carbon ratio (the cool and relatively fresh high-latitude waters) (Key et al., 2004). This biogeochemical gradient results in a high CO_2 buffering capacity of subtropical water, permitting high anthropogenic CO_2 uptake, and a low buffering capacity at higher latitudes, limiting local future CO_2 uptake (Sabine et al., 2004). Combined with the advection of water from the subtropical to subpolar gyre, this latitudinal buffering gradient will likely impact the response of the sink to rising CO_2^{atm} (Volker et al., 2002).

Presently there is no agreement on the relative importance of the different factors described above in controlling past or future subpolar North Atlantic CO_2 uptake

BGD
11, 14551–14585, 2014

change. The hypothesised mechanisms for past decadal to multidecadal timescale changes in subpolar North Atlantic CO_2 uptake fall into four groups:

1. *Biological drawdown*. Evidence that CO_2 uptake variability may arise from the biological transport of carbon out of the surface ocean comes from the relative timing of observed surface ocean pCO_2 and chlorophyll change (Lefèvre et al., 2004). The magnitude of this effect has however been questioned (Bennington et al., 2009).

2. *Temperature*. Both observational and model studies indicate that the temperature dependence of inorganic carbon speciation and CO_2 saturation is likely to have been an important player in air–sea CO_2 flux change on various timescales (Le Quere et al., 2000; Lefèvre et al., 2004; McKinley et al., 2011; Omar and Olsen, 2006; Perez et al., 2013).

3. *Vertical mixing*. Changes in vertical mixing (through deep convection or stratification) has been proposed from both models and observations to be a dominant mechanism for changing the surface total dissolved inorganic carbon (DIC) concentration and DIC-alkalinity ratio, and therefore changing the surface pCO_2 saturation (McKinley et al., 2004; Metzl et al., 2010; Schuster and Watson, 2007; Ullman et al., 2009), although this effect is likely to be damped by the associated changing vertical flux of nutrients and therefore biological CO_2 drawdown (McKinley et al., 2004).

4. *Horizontal advection*. Changes in surface ocean pCO_2 saturation driven by horizontal advection (rather than vertical transport) have been proposed from both modelling and observational studies (Omar and Olsen, 2006; Thomas et al., 2008). Debate however exists about the degree of long term DIC and alkalinity change, which brings in to question mechanisms implicating vertical and/or horizontal DIC and/or alkalinity transport (Corbiere et al., 2007).

BGD
11, 14551–14585, 2014

The diversity of proposed explanations for the observed subpolar North Atlantic CO_2 uptake variability could reflect different mechanisms dominating at different times and influencing uptake over different timescales. Many of the studies to-date have however examined approximately the same time-periods. The range of proposed mechanisms therefore more-likely reflects the difficulty of identifying causal drivers of change in a system, which despite huge effort, is still far from completely observed. Similar problems apply to model-based studies. Proving causality in a model is straight forward when considering drivers external to the system (e.g. rising anthropogenic CO_2 emissions), because those drivers can be switched on and off, but when potentially important components of the mechanism are emergent properties of the model (e.g. the AMOC), these components can not simply be switched on and off, and even where they can be stopped (e.g. in the case of the AMOC by flooding the high-latitude North Atlantic/Arctic with freshwater), their role in the mechanism can not be isolated, because many other factors will change contemporaneously. To understand the mechanisms operating within ESMs, it can therefore often be useful to produce an even simpler model of the system (e.g. Good et al., 2011; Hooss et al., 2001; Meinshausen et al., 2011), one that emulates the complex model's behaviour, but also allows one to separately isolate the different components of the mechanisms. This is particularly valuable when attempting to understand common (or divergent) behaviours across a large suite of models.

Here we explore the mechanisms controlling ocean CO_2 uptake across a large ensemble of HadCM3 (3rd Hadley Centre Climate Model) based ESMs in which parameters have been systematically varied to efficiently sample a wide range of model behaviours (Lambert et al., 2013). We make use of the Atlantic carbon-cycle box model presented by Völker et al., (2002) to emulate the more complex ESM and by dong to simplify this large suite of simulations. The value of simplifying our large suite of ESM simulations in this way is that:

1. By using a single box model that replicates the behaviour of a wide range of Earth System Model formulations using only a single set of parameters (i.e. not retuning

BGD
11, 14551–14585, 2014

the simple model to emulate each different version of the more comprehensive model), one can be confident that the box model contains (and therefore that one has identified) the key processes important to the change of interest within those Earth System Model formulations. I.e. by fitting a small number of parameters within a single box model to a large number of ESM results, one in effect has a highly-constrained set of simultaneous equations describing the system. Almost all of the ESPPE uncertainty is therefore contained within the inputs to the box model rather than the parameters within the box model. The different processes of North Atlantic subpolar CO_2 uptake simulated by ESPPE ensemble members are therefore captured within these box-model inputs.

2. Within a box model one can isolate and quantify the importance of each of these drivers of change by sequentially holding the inputs representing that driver constant and re-running the ensemble. As discussed, this cannot be done in an Earth System Model where properties like overturning circulation emerge from the physics and are therefore impossible to prescribe.

3. Using a box model shown to replicate (without retuning) the behaviour of multiple Earth System Model formulations, one can undertake numerous idealised simulations (e.g. $CO_2^{atm.}$ increasing following various power-law curves), and by doing so develop a thorough understanding of the mechanisms at play. To do this with a full ESM would be extremely time consuming and expensive.

2 Methods

We attempt to isolate the mechanisms controlling North Atlantic CO_2 uptake in a 27 member ESM ensemble based on a carbon cycle version of the 3rd Hadley centre Climate Model HadCM3C (an updated version of Cox et al., 2000, with increased horizontal resolution and improved aerosol representation (Lambert et al., 2013), and using the Hadley centre Ocean Carbon Cycle, HadOCC, sub-model described

BGD
11, 14551–14585, 2014

in Palmer and Totterdell, 2001), in which the atmosphere and ocean physics, the atmospheric sulphur cycle and terrestrial biogeochemistry parameters have been systematically varied to optimally sample parameter space (Lambert et al., 2013). The HadCM3C perturbed parameter ensemble is referred to herein as ESPPE (Earth System Perturbed Parameter Ensemble). The original ESPPE ensemble contains 57 members, but data corruption meant that only 27 of these members could be used in the analysis presented here. The ESPPE ensemble follows the CMIP5 RCP8.5 pathway (Riahi et al., 2007), and has a fully interactive carbon cycle: CO_2 emissions are prescribed, and atmospheric CO_2 concentrations calculated.

The box model we use to simplify the behaviour of the ESPPE represents the major features of the Atlantic basin and Atlantic sector of the Southern Ocean, and is made up of 6 boxes, three surface and three deep. The surface boxes represent the top 300 m of the ocean south of 30° S, the top 150 m of the tropical ocean between 30° S and 48° N, and the upper 300 m of the subpolar region north of 48° N (Fig. 3). The three subsurface boxes represent the deep high-latitude ocean north of 48° N, the intermediate depth ocean between 150 and 1000 m in the tropical region (30° S–48° N), and the remaining deep Atlantic ocean. The volume fluxes between the 6 boxes, and the temperature, salinity and alkalinity of those boxes are prescribed, as is the atmospheric CO_2 concentration. The position and volume of the boxes, the mixing between the boxes, and the way advection is divided between boxes is based on observations and remains unchanged from that described in Völker et al. (2002). The model advects dissolved inorganic carbon (DIC) between boxes in quantities proportional to the prescribed overturning circulation strength, and mixes DIC between vertically adjacent boxes, as described in Völker et al. (2002). The box model does not include any representation of biological carbon fluxes, which were (and are commonly) considered to be of limited importance to anthropogenic carbon uptake (e.g. Volker et al., 2002; Perez et al., 2013). In each of the three surface boxes, the CO_2 concentration is calculated from the DIC, temperature, salinity and alkalinity. Any disequilibrium between partial pressures of CO_2 in the ocean and atmosphere then drives a flux which is rate limited

BGD
11, 14551–14585, 2014

by a prescribed piston velocity. The calculated air–sea CO_2 flux then modifies the concentration of DIC in each box. The formulation of the box model remains exactly as described in Völker et al. (2002) other than the tuning of the box model's parameters (Table 1) to allow the box model to replicate results from the perturbed parameter ensemble. Note that by prescribing changes in alkalinity and allowing the DIC to adjust through air–sea flux, we are implicitly assuming that there is no significant freshwater-driven dilution/concentration of DIC and alkalinity.

To allow the box model to emulate the ESPPE, a single set of box model parameters was obtained by first running a 1000 member box model ensemble in which each of the box model parameters were varied. Parameter space was sampled using a latin hypercube. The fitness of each of the 1000 parameter sets was then judged by calculating the average coefficient of determination (R^2) across the 27 ESPPE members between the ESPPE subpolar gyre air–sea flux, and the box model air–sea flux. The ability of the box model to reproduce the ESM carbon flux is more dependent on the driving time-series ($CO_2^{atm.}$, temperature, salinity, alkalinity and overturning circulation strength) than it is dependent on the exact box model parameters. Indeed the ability of the box model is relatively insensitive to the box model parameters (Fig. 4 and Table 1), suggesting that conclusions drawn on the drivers of the box model CO_2 flux are unlikely to be strongly dependent on the exact choice of box model parameters. The six parameter sets that gave the highest R^2 when compared with ESPPE output are presented in Table 2.

Variability on different timescales is separated using high and low-pass filtering. Filtering is achieved by applying a 5th order Butterworth fast Fourier transform filter. The mechanisms driving the modes of variability isolated using the high and low-pass filters are identified by manipulating the input time-series (temperature, salinity, alkalinity, atm. CO_2 and AMOC strength) used to force the box-model. These input time-series are either filtered, held at a constant value, or left unchanged when supplied to the box-model. Initially only one input time-series is manipulated at a time.

BGD
11, 14551–14585, 2014

In subsequent analysis, multiple input time-series are manipulated to examine their additive effect on the air–sea CO_2 flux.

3 Results and discussion

Using only a single set of parameters, the box model captures much of the variability in subpolar North Atlantic air–sea CO_2 flux simulated within and across the diverse ESPPE members (see examples in Fig. 4 and full dataset in Fig. 5a). This gives us confidence that the box model represents all of the 1st order processes involved in the ESM simulation of North Atlantic CO_2 uptake, and provides us with a diagnostic tool to identify what drives CO_2 uptake variability in the ESPPE.

To explore the mechanisms behind the ESM's variability we initially broke-down the subpolar North Atlantic air–sea flux behaviour simulated within the Earth System Model ensemble by applying high and low pass filters to the data (Fig. 6). This allows us to identify discreet time-scales of variability common across all ensemble members. We find that filtering the ESM results at < 5 years and > 30 years allows us to capture almost all of the ESM's variability whilst cleanly separating the variability in to two components (Fig. 6). We will explore the mechanisms behind these two timescales of variability independently,

To pick apart the contribution of different processes to the high and low frequency air–sea CO_2 flux simulated by the ESPPE, we sequentially control the inputs to the box model, isolating the role of that input in producing the overall change. Firstly, to understand the mechanism behind the high-frequency variability, we high-pass all of the inputs to the box model (temperature, salinity, alkalinity, atmospheric CO_2 concentrations and overturning circulation strength), adding to this the mean value from the original time-series (since the high-pass filtering results in a time-series vary around zero). This process removes any low-frequency variability. The high-pass filtered time-series' are used to drive the box model, and results compared to high-pass filtered results from the ESPPE (Fig. 7). The input variables for the North Atlantic are then

BGD
11, 14551–14585, 2014

sequentially held at their mean value (i.e. removing any variability) and the box model re-run (Fig. 7). To understand the mechanisms driving the low-frequency variability the box model input time-series are sequentially low-pass filtered (all other time-series remain unchanged) and the box model run (Fig. 8).

Splitting the ESPPE North Atlantic subpolar air–sea CO_2 flux into a high and low frequency component a number of things become clear. Firstly, the majority of the total signal can be described by these two separate components (Fig. 6). Secondly, we see that the high frequency component occurs with little coherent structure across all ensemble members, but it does show an increase in variability towards 2100 (Fig. 6). Thirdly, we see that the low-period signal tends to increase from its pre-industrial value through the 20th Century, then in most cases peaks during the 21st Century, then begins to decline (Fig. 6).

The "peak and decline" behaviour seen in the low-frequency air–sea CO_2 flux signal is unlike the globally averaged signal (Fig. 2), which under a CO_2 emission scenario like RCP8.5 (in which atmospheric concentrations are increasing throughout the 21st Century) would be expected to (and indeed does: Fig. 2) continue increasing, but at a progressively reduced rate. As long as the atmospheric CO_2 concentration is increasing, assuming no dramatic changes in ocean circulation or biology, there will always be an air to sea CO_2 concentration gradient, and therefore air-to-sea CO_2 flux. The decrease in this flux through time reflects the changing speciation of carbon in seawater in response to the increase in carbonic acid concentrations – which partitions carbon progressively in the direction of CO_2, elevating surface ocean CO_2 concentrations, and reducing the air–sea CO_2 concentration gradient (Zeebe and Wolf-Gladrow, 2001; Revelle and Suess, 1957).

The difference in behaviour between the subpolar North Atlantic and the well understood chemical response of the steady-state ocean (Revelle and Suess, 1957) (as largely seen here in the global average: Fig. 2) indicates that CO_2 emission (and potentially associated climate change) forced physical, biological or chemical changes in the North Atlantic are modifying the capacity of this sink to take up atmospheric

BGD
11, 14551–14585, 2014

CO_2. "Peak and decline" North Atlantic CO_2 uptake has previously been identified in an idealised study by Völker et al. (2002) (using the box-model applied in this study), who demonstrated theoretically that the subpolar region could take up less atmospheric CO_2 in the future than it did in the preindustrial, without invoking any change in ocean circulation or biology. The "peak and decline" demonstrated by Völker et al. (2002) occurred in response to proportionally more CO_2 being taken up under higher atmospheric CO_2 conditions in the subtropical than subpolar North Atlantic – in response to the higher alkalinity (and therefore lower Revelle Factor (Revelle and Suess, 1957) and higher buffering of surface ocean pCO_2) in the subtropical waters, and that excess carbon being transported north into the subpolar gyre by the overturning circulation (explained further in Fig. 9 and caption).

3.1 Drivers of multidecadal/centenial behaviour

To assess the drivers of multidecadal/centenial variability, we first plot each annual-average value from the ESM simulations against the equivalent value generated using the box model (Fig. 5a). We then sequentially apply a low-pass filter to each input variable (and sets of input variables) to remove the low-frequency (> 30 year) variability from that/those input variable/variables, and using those input values run the box model. We then examine how the removal of low-frequency variability from the different input variables changes the output of the box model (Fig. 5b).

We find that the most important driver of the low-frequency ("peak and decline") variability in the subpolar North Atlantic air–sea CO_2 flux comes from the progressive increase in atmospheric CO_2 concentrations (Fig. 5), which drives much of both the increase and decrease (Fig. 8) in CO_2 flux, as described under idealised conditions by Völker et al. (2002). It is clear however that without a low-frequency signal in the atmospheric CO_2 concentrations fed into the box model, a 21st Century decline in air–sea CO_2 flux is still present. This secondary decline is driven by a slow reduction in subpolar alkalinity and to a lesser degree warming (Figs. 5 and 10). This finding

BGD
11, 14551–14585, 2014

confirms the applicability of the idea proposed by Völker et al. (2002), and described in the proceeding paragraph, to our ESM ensemble (Fig. 5).

The similarity between the box model behaviour with no filtered inputs (i.e. optimally emulating the ESPPE), and with input salinity and AMOC filtered (Fig. 5), tells us that these two factors are not having an important impact on the low-frequency subpolar North Atlantic "peak and decline" air–sea flux time evolution (Fig. 5). Removing the low-frequency signal from the temperature time-series used by the box model has a minor effect (Fig. 5), causing the box model to over-predict the air–sea CO_2 flux at times of high flux, which translates in time-series analysis to slightly underestimating the decline (Fig. 8). Similarly removing the low-frequency signal from the alkalinity time-series input to the box model causes a slightly greater over-prediction of air–sea CO_2 flux values during the decline phase (Figs. 5 and 8).

3.2 Drivers of annual/interannual behaviour

Moving now to the high-frequency variability simulated within the ESPPE (Fig. 7), we compare box model simulations run with all input time-series high-pass filtered, with high-pass filtered ESPPE subpolar North Atlantic air–sea CO_2 flux data. We then sequentially (and then together) hold the input time-series constant at their average values (Fig. 11), and re-run the box model to isolate the contribution of variability in each of the input time-series to ESPPE result. We find that the box model captures the temporal variability but tends to underestimate the magnitude of variability (Fig. 11a). Holding temperature and alkalinity (yellow dots) constant we find near-complete breakdown of the box model's ability to capture the ESM's CO_2 flux variability (Fig. 11b). Independently holding temperature and alkalinity constant we find that these factors separately account for much of the correlation between the box model and ESPPE high-frequency variability. Holding salinity, meridional overturning circulation strength and atmospheric CO_2 concentrations constant (in turn) we find little impact on the correlation between the box model and the ESSPE results (Fig. 11b). It is therefore clear that the high-frequency variability simulated by the ESM within the

BGD
11, 14551–14585, 2014

ESPPE is almost completely driven by variability in temperature and alkalinity, and is largely insensitive to the models' variability in salinity, AMOC and atmospheric CO_2 on these timescales.

4 Conclusions

We find very different mechanisms are controlling the interannual and centennial subpolar North Atlantic CO_2 variability in our large ensemble of perturbed parameter ESM simulations. The interannual variability is controlled by rapid changes in the local seawater temperature and alkalinity fields, whereas the centennial variability is largely controlled by the time-evolution of atmospheric CO_2 concentrations interacting with the background chemical gradient (high to low alkalinity) and carbon transport moving northwards up the Atlantic, with secondary and tertiary effects from alkalinity and temperature change respectively. Here we see both how increasing atmospheric CO_2 concentrations can have an unintuitive and complex impact on the subpolar North Atlantic sink, and how alkalinity can modify this behaviour.

Our findings suggest that while it is important to understand the mechanisms behind recent interannual variability in the subpolar North Atlantic CO_2 flux, that understanding might not directly inform us about how the sink is likely to change in the future. The fact that the future strength of the subpolar North Atlantic CO_2 sink appears to be largely controlled by the basic chemical response of seawater to rising atmospheric CO_2 concentrations (rather than physical or biological components of the model – in which we would have less confidence) gives us reason to consider it likely that this behaviour could be shared by the real-world future ocean. This raises the question, if the real-world North Atlantic CO_2 sink is to follow this peak and decline trajectory, where on this trajectory do we presently sit? Perhaps the suggestion that the strength of the subpolar North Atlantic CO_2 sink has been decreasing (e.g. McKinley et al., 2011; Schuster and Watson, 2007) indicates that the real-world system is already in long-term decline.

BGD
11, 14551–14585, 2014

Acknowledgements. This work was supported by the EU FP7 Collaborative Project CarboOcean (Grant Agreement Number 264879), the Joint DECC/Defra Met Office Hadley Centre Climate Programme (GA01101), and the NERC directed research programme RAGNARoCC (NE/K002473/1).

References

Bennington, V., McKinley, G. A., Dutkiewicz, S., and Ulman, D.: What does chlorophyll variability tell us about export and air–sea CO_2 flux variability in the North Atlantic?, Global Biogeochem. Cy., 23, GB3002, doi:10.1029/2008GB003241, 2009. 14555

Booth, B. B. B., Jones, C. D., Collins, M., Totterdell, I. J., Cox, P. M., Sitch, S., Huntingford, C., Betts, R. A., Harris, G. R., and Lloyd, J.: High sensitivity of future global warming to land carbon cycle processes, Environ. Res. Lett., 7, 024002, doi:10.1088/1748-9326/7/2/024002, 2012. 14553

Carr, M.-E., Friedrichs, M. A. M., Schmeltz, M., Aita, M. N., Antoine, D., Arrigo, K. R., Asanuma, I., Aumont, O., Barber, R., Behrenfeld, M., Bidigare, R., Buitenhuis, E. T., Campbell, J., Ciotti, A., Dierssen, H., Dowell, M., Dunne, J., Esaias, W., Gentili, B., Gregg, W., Groom, S., Hoepffner, N., Ishizaka, J., Kameda, T., Le Quere, C., Lohrenz, S., Marra, J., Melin, F., Moore, K., Morel, A., Reddy, T. E., Ryan, J., Scardi, M., Smyth, T., Turpie, K., Tilstone, G., Waters, K., and Yamanaka, Y.: A comparison of global estimates of marine primary production from ocean color, Deep-Sea Res. Pt. II, 53, 741–770, doi:10.1016/j.dsr2.2006.01.028, 2006. 14554

Corbiere, A., Metzl, N., Reverdin, G., Brunet, C., and Takahashi, A.: Interannual and decadal variability of the oceanic carbon sink in the North Atlantic subpolar gyre, Tellus B, 59, 168–178, doi:10.1111/j.1600-0889.2006.00232.x, 2007. 14555

Cox, P., Betts, R., Jones, C., Spall, S., and Totterdell, I.: Acceleration of global warming due to carbon-cycle feedbacks in a coupled climate model, Nature, 408, 184–187, doi:10.1038/35041539, 2000. 14557

Friedlingstein, P., Cox, P., Betts, R., Bopp, L., Von Bloh, W., Brovkin, V., Cadule, P., Doney, S., Eby, M., Fung, I., Bala, G., John, J., Jones, C., Joos, F., Kato, T., Kawamiya, M., Knorr, W., Lindsay, K., Matthews, H. D., Raddatz, T., Rayner, P., Reick, C., Roeckner, E., Schnitzler, K. G., Schnur, R., Strassmann, K., Weaver, A. J., Yoshikawa, C., and

BGD
11, 14551–14585, 2014

Zeng, N.: Climate-carbon cycle feedback analysis: results from the (CMIP)-M-4 model intercomparison, J. Climate, 19, 3337–3353, doi:10.1175/JCLI3800.1, 2006. 14553

Good, P., Gregory, J. M., and Lowe, J. A.: A step-response simple climate model to reconstruct and interpret AOGCM projections, Geophys. Res. Lett., 38, L01703, doi:10.1029/2010GL045208, 2011. 14556

Halloran, P. R.: Does atmospheric CO_2 seasonality play an important role in governing the air-sea flux of CO_2?, Biogeosciences, 9, 2311–2323, doi:10.5194/bg-9-2311-2012, 2012. 14553

Hooss, G., Voss, R., Hasselmann, K., Maier-Reimer, E., and Joos, F.: A nonlinear impulse response model of the coupled carbon cycle-climate system (NICCS), Clim. Dynam., 18, 189–202, doi:10.1007/s003820100170, 2001. 14556

Ito, T., Woloszyn, M., and Mazloff, M.: Anthropogenic carbon dioxide transport in the Southern Ocean driven by Ekman flow, Nature, 463, 80–U85, doi:10.1038/nature08687, 2010. 14553

Jones, C., Robertson, E., Arora, V., Friedlingstein, P., Shevliakova, E., Bopp, L., Brovkin, V., Hajima, T., Kato, E., Kawamiya, M., Liddicoat, S., Lindsay, K., Reick, C. H., Roelandt, C., Segschneider, J., and Tjiputra, J.: Twenty-first-century compatible CO_2 emissions and airborne fraction simulated by CMIP5 earth system models under four representative concentration pathways, J. Climate, 26, 4398–4413, doi:10.1175/JCLI-D-12-00554.1, 2013. 14553

Key, R. M., Kozyr, A., Sabine, C. L., Lee, K., Wanninkhof, R., Bullister, J. L., Feely, R., Millero, F. J., Mordy, C., and Peng, T.-H.: A global ocean carbon climatology: Results from Global Data Analysis Project (GLODAP), Global Biogeochem. Cy., 18, GB4031, doi:10.1029/2004GB002247, 2004. 14554

Lambert, F., Harris, G., Collins, M., Murphy, J., Sexton, D., and Booth, B.: Interactions between perturbations to different Earth system components simulated by a fully-coupled climate model, Clim. Dynam., 41, 3055–3072, doi:10.1007/s00382-012-1618-3, 2013. 14556, 14557, 14558

Le Quere, C., Orr, J., Monfray, P., Aumont, O., and Madec, G.: Interannual variability of the oceanic sink of CO_2 from 1979 through 1997, Global Biogeochem. Cy., 14, 1247–1265, 2000. 14555

Le Quere, C., Roedenbeck, C., Buitenhuis, E. T., Conway, T. J., Langenfelds, R., Gomez, A., Labuschagne, C., Ramonet, M., Nakazawa, T., Metzl, N., Gillett, N., and Heimann, M.: Saturation of the Southern Ocean CO_2 sink due to recent climate change, Science, 316, 1735–1738, doi:10.1126/science.1136188, 2007. 14553

BGD
11, 14551–14585, 2014

Lefèvre, N., Watson, A., Olsen, A., Ríos, A., Pérez, F., and Johannessen, T.: A decrease in the sink for atmospheric CO_2 in the North Atlantic, Geophys. Res. Lett., 31, L07306, doi:10.1029/2003GL018957, 2004. 14555

Lenton, A. and Matear, R. J.: Role of the Southern Annular Mode (SAM) in Southern Ocean CO_2 uptake, Global Biogeochem. Cy., 21, GB2016, doi:10.1029/2006GB002714, 2007. 14553

Lenton, A., Codron, F., Bopp, L., Metzl, N., Cadule, P., Tagliabue, A., and Le Sommer, J.: Stratospheric ozone depletion reduces ocean carbon uptake and enhances ocean acidification, Geophys. Res. Lett., 36, L12606, doi:10.1029/2009GL038227, 2009. 14553

Lovenduski, N. S., Long, M. C., Gent, P. R., and Lindsay, K.: Multi-decadal trends in the advection and mixing of natural carbon in the Southern Ocean, Geophys. Res. Lett., 40, 139–142, doi:10.1029/2012GL054483, 2013. 14553

Marinov, I., Gnanadesikan, A., Sarmiento, J. L., Toggweiler, J. R., Follows, M., and Mignone, B. K.: Impact of oceanic circulation on biological carbon storage in the ocean and atmospheric $pCO_(2)$, Global Biogeochem. Cy., 22, GB3007, doi:10.1029/2007GB002958, 2008. 14553

McKinley, G., Follows, M., and Marshall, J.: Mechanisms of air–sea CO_2 flux variability in the equatorial Pacific and the North Atlantic, Global Biogeochem. Cy., 18, GB2011, doi:10.1029/2003GB002179, 2004. 14553, 14555

McKinley, G. A., Fay, A. R., Takahashi, T., and Metzl, N.: Convergence of atmospheric and North Atlantic carbon dioxide trends on multidecadal timescales, Nat. Geosci., 4, 606–610, doi:10.1038/ngeo1193, 2011. 14553, 14554, 14555, 14564

Meinshausen, M., Wigley, T. M. L., and Raper, S. C. B.: Emulating atmosphere-ocean and carbon cycle models with a simpler model, MAGICC6 – Part 2: Applications, Atmos. Chem. Phys., 11, 1457–1471, doi:10.5194/acp-11-1457-2011, 2011. 14556

Metzl, N., Corbiere, A., Reverdin, G., Lenton, A., Takahashi, T., Olsen, A., Johannessen, T., Pierrot, D., Wanninkhof, R., Olafsdottir, S. R., Olafsson, J., and Ramonet, M.: Recent acceleration of the sea surface fCO(2) growth rate in the North Atlantic subpolar gyre (1993–2008) revealed by winter observations, Global Biogeochem. Cy., 24, GB4004, doi:10.1029/2009GB003658, 2010. 14553, 14555

Murnane, R., Sarmiento, J., and Le Quere, C.: Spatial distribution of air–sea CO(2) fluxes and the interhemispheric transport of carbon by the oceans, Global Biogeochem. Cy., 13, 287–305, doi:10.1029/1998GB900009, 1999. 14553

BGD
11, 14551–14585, 2014

Omar, A. and Olsen, A.: Reconstructing the time history of the air–sea CO_2 disequilibrium and its rate of change in the eastern subpolar North Atlantic, 1972–1989, Geophys. Res. Lett., 33, L04602, doi:10.1029/2005GL025425, 2006. 14555

Palmer, J. and Totterdell, I.: Production and export in a global ocean ecosystem model, Deep-Sea Res. Pt. I, 48, 1169–1198, doi:10.1016/S0967-0637(00)00080-7, 2001. 14558

Perez, F. F., Mercier, H., Vazquez-Rodriguez, M., Lherminier, P., Velo, A., Pardo, P. C., Roson, G., and Rios, A. F.: Atlantic Ocean CO_2 uptake reduced by weakening of the meridional overturning circulation, Nat. Geosci., 6, 146–152, doi:10.1038/NGEO1680, 2013. 14553, 14555, 14558

Rayner, N., Parker, D., Horton, E., Folland, C., Alexander, L., Rowell, D., Kent, E., and Kaplan, A.: Global analyses of sea surface temperature, sea ice, and night marine air temperature since the late nineteenth century, J. Geophys. Res., 108, 4407, doi:10.1029/2002JD002670, 2003. 14554

Revelle, R. and Suess, H. E.: Carbon dioxide exchange between atmosphere and ocean and the question of an increase of atmospheric CO_2 during the past decades, Tellus, 9, 18–27, doi:10.1111/j.2153-3490.1957.tb01849.x, 1957. 14561, 14562

Riahi, K., Gruebler, A., and Nakicenovic, N.: Scenarios of long-term socio-economic and environmental development under climate stabilization, Technol. Forecast. Soc., 74, 887–935, 2007. 14558

Roy, T., Bopp, L., Gehlen, M., Schneider, B., Cadule, P., Froelicher, T. L., Segschneider, J., Tjiputra, J., Heinze, C., and Joos, F.: Regional impacts of climate change and atmospheric CO_2 on future ocean carbon uptake: a multimodel linear feedback analysis, J. Climate, 24, 2300–2318, doi:10.1175/2010JCLI3787.1, 2011. 14553

Russell, J. L., Dixon, K. W., Gnanadesikan, A., Stouffer, R. J., and Toggweiler, J. R.: The Southern Hemisphere westerlies in a warming world: propping open the door to the deep ocean, J. Climate, 19, 6382–6390, doi:10.1175/JCLI3984.1, 2006. 14553

Sabine, C., Feely, R., Gruber, N., Key, R., Lee, K., Bullister, J., Wanninkhof, R., Wong, C., Wallace, D., Tilbrook, B., Millero, F., Peng, T., Kozyr, A., Ono, T., and Rios, A.: The oceanic sink for anthropogenic CO_2, Science, 305, 367–371, doi:10.1126/science.1097403, 2004. 14554

Sallee, J.-B., Matear, R. J., Rintoul, S. R., and Lenton, A.: Localized subduction of anthropogenic carbon dioxide in the Southern Hemisphere oceans, Nat. Geosci., 5, 579–584, doi:10.1038/NGEO1523, 2012. 14553

BGD
11, 14551–14585, 2014

Sarmiento, J. and LeQuere, C.: Oceanic carbon dioxide uptake in a model of century-scale global warming, Science, 274, 1346–1350, doi:10.1126/science.274.5291.1346, 1996. 14553

Schuster, U. and Watson, A. J.: A variable and decreasing sink for atmospheric CO_2 in the North Atlantic, J. Geophys. Res., 112, C11006, doi:10.1029/2006JC003941, 2007. 14553, 14555, 14564

Schuster, U., McKinley, G. A., Bates, N., Chevallier, F., Doney, S. C., Fay, A. R., González-Dávila, M., Gruber, N., Jones, S., Krijnen, J., Landschützer, P., Lefèvre, N., Manizza, M., Mathis, J., Metzl, N., Olsen, A., Rios, A. F., Rödenbeck, C., Santana-Casiano, J. M., Takahashi, T., Wanninkhof, R., and Watson, A. J.: An assessment of the Atlantic and Arctic sea–air CO_2 fluxes, 1990–2009, Biogeosciences, 10, 607–627, doi:10.5194/bg-10-607-2013, 2013. 14554

Seferian, R., Iudicone, D., Bopp, L., Roy, T., and Madec, G.: Water mass analysis of effect of climate change on air–sea CO_2 fluxes: the Southern Ocean, J. Climate, 25, 3894–3908, doi:10.1175/JCLI-D-11-00291.1, 2012. 14553

Takahashi, T., Sutherland, S. C., Wanninkhof, R., Sweeney, C., Feely, R. A., Chipman, D. W., Hales, B., Friederich, G., Chavez, F., Sabine, C., Watson, A., Bakker, D. C. E., Schuster, U., Metzl, N., Yoshikawa-Inoue, H., Ishii, M., Midorikawa, T., Nojiri, Y., Koertzinger, A., Steinhoff, T., Hoppema, M., Olafsson, J., Arnarson, T. S., Tilbrook, B., Johannessen, T., Olsen, A., Bellerby, R., Wong, C. S., Delille, B., Bates, N. R., and de Baar, H. J. W.: Climatological mean and decadal change in surface ocean pCO(2), and net sea–air CO_2 flux over the global oceans, Deep-Sea Res. Pt. II, 56, 554–577, doi:10.1016/j.dsr2.2008.12.009, 2009. 14554

Taylor, K. E., Stouffer, R. J., and Meehl, G. A.: An overview of CMIP5 and the experiment design, B. Am. Meteorol. Soc., 93, 485–498, doi:10.1175/BAMS-D-11-00094.1, 2012. 14553

Thomas, H., Prowe, A. E. F., Lima, I. D., Doney, S. C., Wanninkhof, R., Greatbatch, R. J., Schuster, U., and Corbiere, A.: Changes in the North Atlantic Oscillation influence CO_2 uptake in the North Atlantic over the past 2 decades, Global Biogeochem. Cy., 22, GB4027, doi:10.1029/2007GB003167, 2008. 14553, 14555

Ullman, D. J., McKinley, G. A., Bennington, V., and Dutkiewicz, S.: Trends in the North Atlantic carbon sink: 1992–2006, Global Biogeochem. Cy., 23, GB4011, doi:10.1029/2008GB003383, 2009. 14553, 14555

BGD
11, 14551–14585, 2014

Verdy, A., Dutkiewicz, S., Follows, M. J., Marshall, J., and Czaja, A.: Carbon dioxide and oxygen fluxes in the Southern Ocean: mechanisms of interannual variability, Global Biogeochem. Cy., 21, GB2020, doi:10.1029/2006GB002916, 2007. 14553

Volker, C., Wallace, D., and Wolf-Gladrow, D.: On the role of heat fluxes in the uptake of anthropogenic carbon in the North Atlantic, Global Biogeochem. Cy., 16, 1138, doi:10.1029/2002GB001897, 2002. 14554, 14556, 14558, 14559, 14562, 14563, 14583

Volodin, E. M., Dianskii, N. A., and Gusev, A. V.: Simulating present-day climate with the INMCM4.0 coupled model of the atmospheric and oceanic general circulations, Izv. Atmos. Ocean. Phy.+, 46, 414–431, doi:10.1134/S000143381004002X, 2010. 14553

Watson, A. J., Schuster, U., Bakker, D. C. E., Bates, N. R., Corbiere, A., Gonzalez-Davila, M., Friedrich, T., Hauck, J., Heinze, C., Johannessen, T., Koertzinger, A., Metzl, N., Olafsson, J., Olsen, A., Oschlies, A., Antonio Padin, X., Pfeil, B., Magdalena Santana-Casiano, J., Steinhoff, T., Telszewski, M., Rios, A. F., Wallace, D. W. R., and Wanninkhof, R.: Tracking the Variable North Atlantic Sink for Atmospheric CO_2, Science, 326, 1391–1393, doi:10.1126/science.1177394, 2009. 14554

Zeebe, R. and Wolf-Gladrow, D.: CO_2 in Seawater: Equilibrium, Kinetics, Isotopes, Elsevier Oceanography Book Series, Amsterdam, 2001. 14554, 14561

BGD
11, 14551–14585, 2014

Table 1. Parameters used in box model.

Parameter name	Parameter value	Parameter description
T	variable	overturning circulation strength (Sv)
a	7/14	fraction of overturning circulation strength
b	2/14	fraction of overturning circulation strength
mix_{eq}	variable	vertical mixing (Sv)
$\text{mix}_{\text{north}}$	variable	vertical mixing (Sv)
$\text{flux}_{\text{south}}$	variable	southern box piston velocity (m h^{-1})
flux_{eq}	variable	equatorial box piston velocity (m h^{-1})
$\text{flux}_{\text{north}}$	variable	northern box piston velocity (m h^{-1})

BGD
11, 14551–14585, 2014

Table 2. Box model parameter values.

Ranking	Parameter						
	piston (Sp)	piston (S)	piston (Eq)	mix_{eq}	mix_{north}	alpha	beta
1st	0.177	0.0854	0.142	1.02	2.09	0.286	0.0103
2nd	0.168	0.138	0.211	19.2	12.7	5.37×10^{-3}	8.72×10^{-2}
3rd	2.82×10^{-2}	0.321	0.129	13.1	17.1	1.16×10^{-2}	0.727
4th	0.130	0.399	1.56×10^{-3}	6.76	8.65	0.423	2.42×10^{-2}
5th	8.56×10^{-2}	0.199	0.104	8.33	1.09	2.22×10^{-3}	8.60×10^{-2}
6th	0.159	0.0632	0.0136	10.9	13.1	0.608	0.288

BGD
11, 14551–14585, 2014

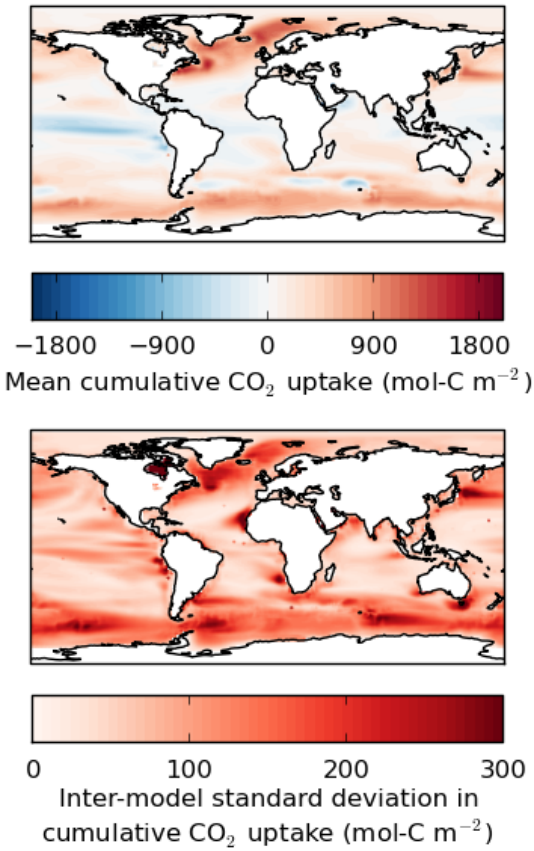

Figure 1. Cumulative sum of air–sea CO_2 flux between the years 1860 and 2100 (RCP8.5). **(a)** Mean and **(b)** inter-model SD across ESPPE.

BGD
11, 14551–14585, 2014

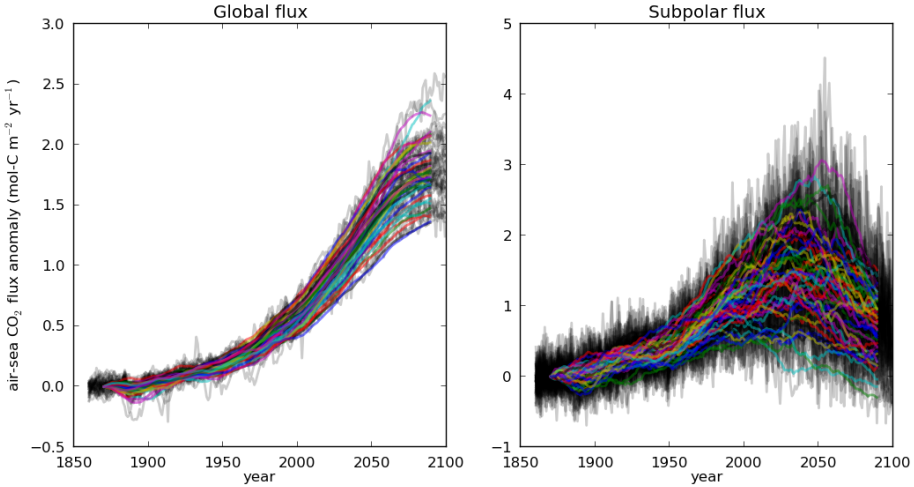

Figure 2. Globally averaged air–sea CO_2 flux across all ESPPE members. Presented as anomaly from 1st 20 years.

BGD
11, 14551–14585, 2014

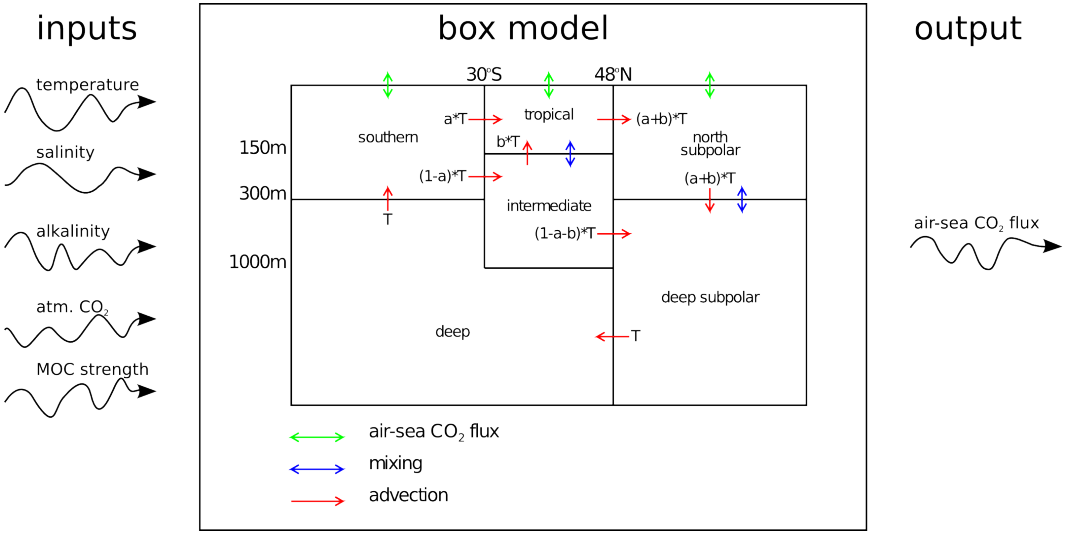

Figure 3. Schematic description of the box model.

BGD
11, 14551–14585, 2014

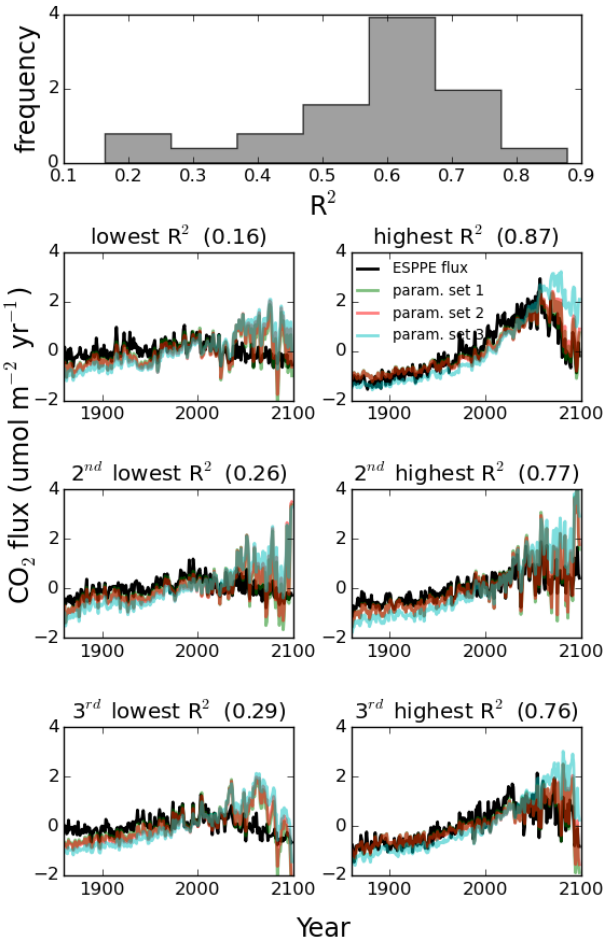

BGD
11, 14551–14585, 2014

Figure 4. Top: histogram showing the distribution of R^2 values describing the relationship between box-model and ESM simulations for each of the 27 ensemble members (using parameter set 1). Lower plots: subpolar North Atlantic air–sea flux simulated within the ESPPE (grey), and emulation of that flux within the box model using the three parameter sets resulting in the lowest mean R^2 value (Table 2) displayed in green, red and blue in order of decreasing mean R^2. The three ensemble members displaying the highest R^2 between ESSPE and box model with parameter set 1, and the three ensemble members displaying the lowest R^2 between ESSPE and box model with parameter set 1 are displayed on the right and left with the best (worst) fit at the top. We highlight the difference in goodness of fit between best and worst situations to demonstrate that it is small compared to common behaviour – i.e. the behaviour that we are trying to understand.

BGD
11, 14551–14585, 2014

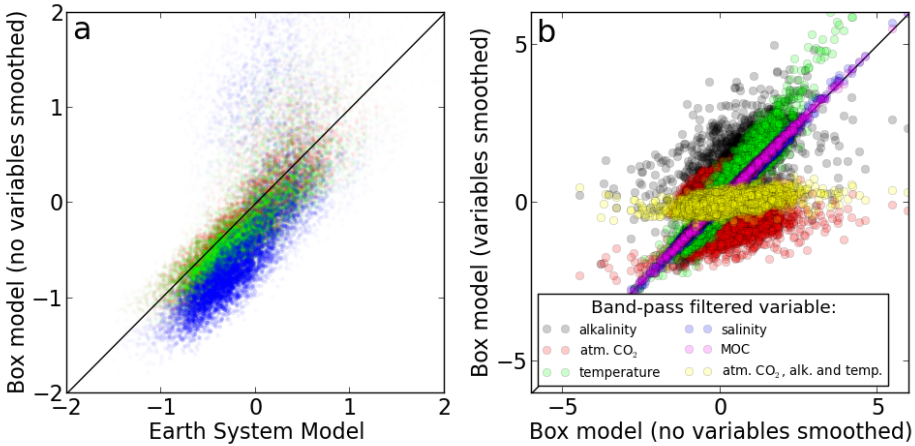

Figure 5. (a) ESPPE subpolar North Atlantic air–sea CO_2 flux plotted against box model estimates of that same flux using the top three box model parameter sets (Table 2) in red, blue and green respectively. **(b)** Results from box model driven with low-frequency variability in all input variables, plotted against: box model results when low-frequency alkalinity signal is removed (black), low-frequency atm. CO_2 signal removed (red), low-frequency temperature signal removed (green), low-frequency salinity signal removed (blue), low-frequency meridional overturning circulation (MOC) signal removed (purple), and low-frequency atmospheric CO_2 concentration, alkalinity and temperature signals all removed (yellow). The straight line represents the one-to-one line upon which results would fall if removal of the low-frequency variability in that variable did not influence CO_2 uptake.

BGD
11, 14551–14585, 2014

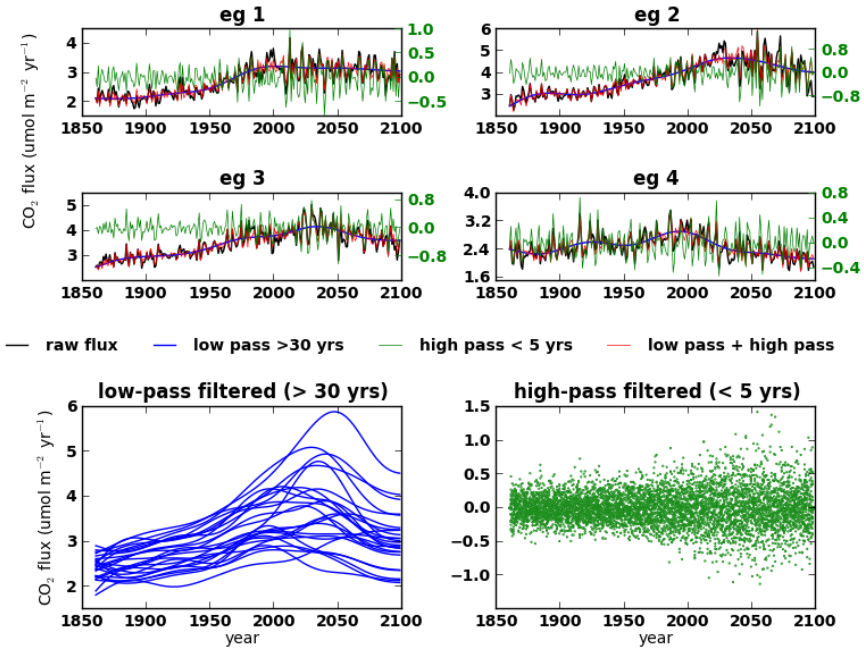

Figure 6. High and low pass filters are applied to the ESPPE subpolar North Atlantic air–sea CO_2 flux simulations to identify the separate time-scales of variability. Top panel: four random ensemble members' CO_2 flux is presented (black) alongside the low-pass (blue) and high-pass (green) processed fluxes. In red, the low and high pass filtered data are recombined to demonstrate that these timescales of variability together explain almost all of the original variability. Lower panel: the low-pass (blue, left) and high-pass (green, right) filtered results across all ensemble members are presented, demonstrating, in the case of the low-pass filters results, great diversity in model evolution.

BGD
11, 14551–14585, 2014

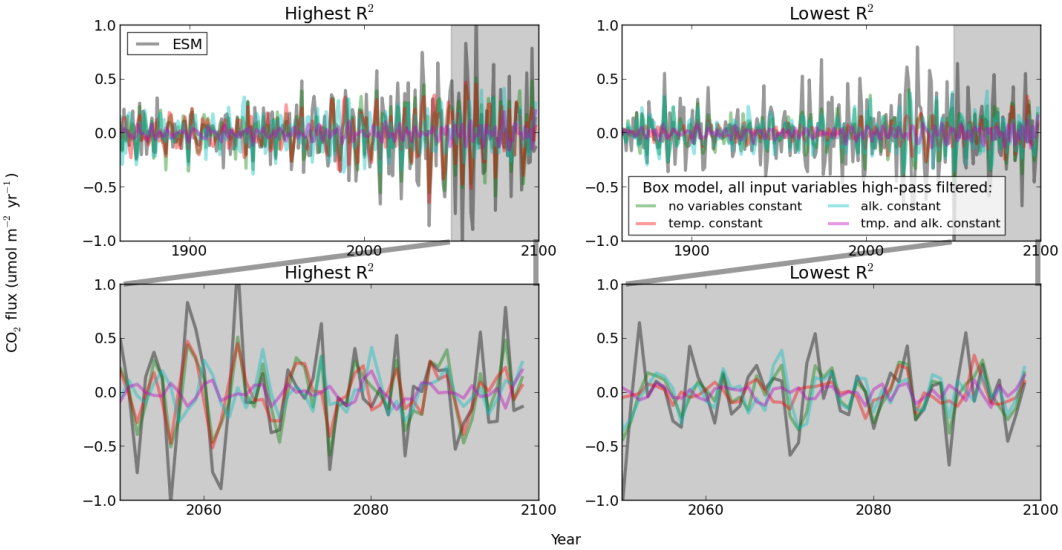

Figure 7. Illustration of the fit (best and worst case as assessed by R^2) between high-pass filtered ESPPE North Atlantic subpolar gyre air–sea CO_2 flux and the box model results when driven with high-pass filtered input time-series. Similarity between the dark blue (ESPPE subpolar North Atlantic air–sea CO_2 flux) and green lines illustrates the box model's ability to capture high frequency variability in the ESM ensemble. Red, light blue and purple lines show how the box-model's fit to the ESPPE's high-frequency subpolar North Atlantic air–sea CO_2 flux variability is dependant on temperature and alkalinity. Factors other than temperature and alkalinity do not play an important role in variability on this timescale (Fig. 11) so have been excluded from this figure for clarity.

BGD
11, 14551–14585, 2014

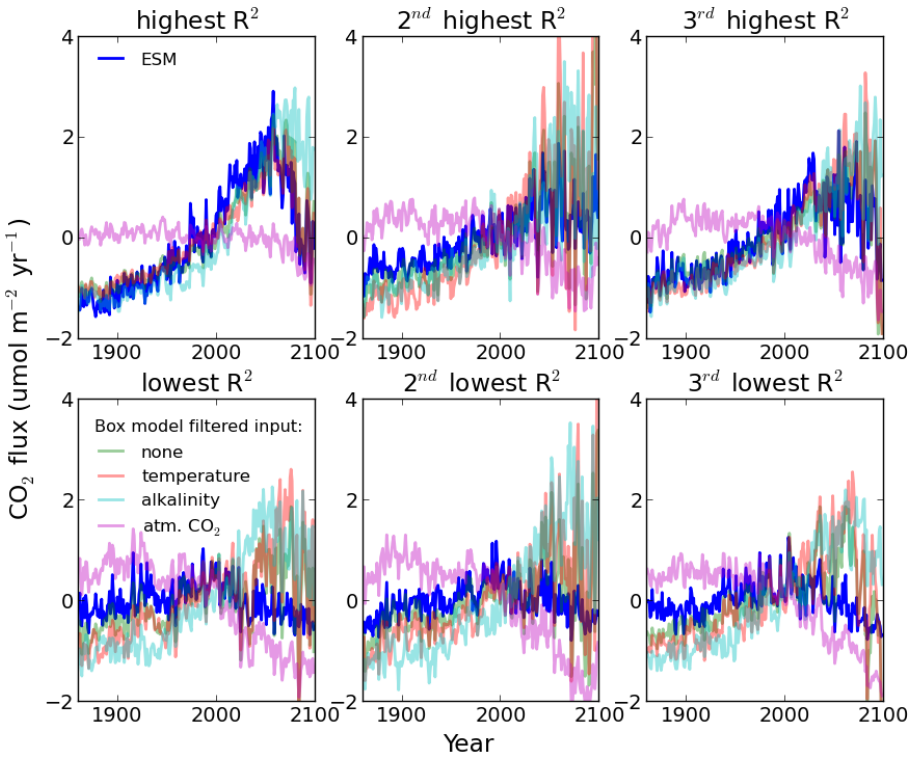

Figure 8. Illustration of the fit (three best and worst case ensemble members as assessed by R^2) between low-pass filtered ESPPE North Atlantic subpolar Gyre air–sea CO_2 flux and the box model results when driven with individual input time-series which have been high-pass filtered. Similarity between the dark blue and green lines highlights the box model's ability to replicate the ESM ensemble's behaviour. Further colours illustrate the dependance of that fit on the time-evolution of the various input variables.

BGD
11, 14551–14585, 2014

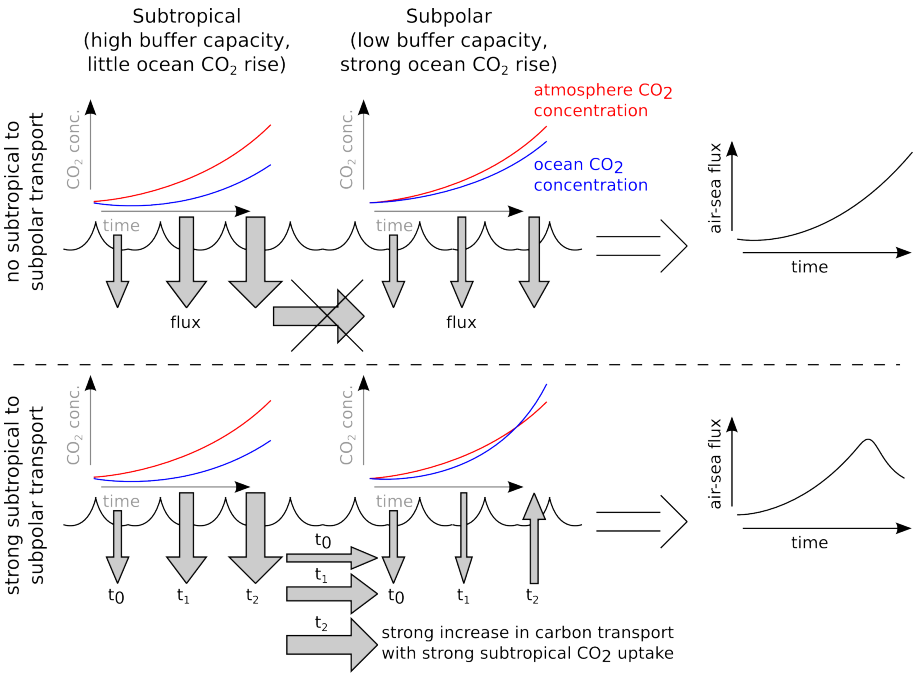

BGD
11, 14551–14585, 2014

Figure 9. Diagrammatic explanation of the mechanism proposed in Völker at al. (2002) by which subpolar North Atlantic CO_2 concentration may peak then decline in response to continuously rising atmospheric CO_2 concentrations. The top half of the diagram explains what would happen if the subtropical and subpolar Atlantic were not connected by the circulation of the ocean (AMOC). Here, the higher alkalinity to dissolved-carbon ratio (the warm and saline low-latitude waters) of the subtropics means that these waters can strongly take up anthropogenic CO_2 without a big rise in surface ocean CO_2 concentrations. Similarly the higher latitude subpolar waters (with low alkalinity to dissolved-carbon ratios) continuously take up CO_2, but the (relatively) small buffering capacity of these waters means that the surface ocean CO_2 concentration rises (relatively) quickly. A smaller air–sea CO_2 gradient is therefore maintained, and the air–sea CO_2 flux is (relatively) small. The bottom half of the diagram represents the situation in the real ocean, and the simulations considered in this study. Here the subtropical and subpolar Atlantic are linked by the near-surface limb of the Atlantic Meridional Overturning Circulation. In this situation, in response to rising atmospheric CO_2, the subtropical CO_2 uptake continues (in our idealised example) as in the top half of the diagram, but some of that that extra carbon is being moved into the subpolar Atlantic, where the buffering capacity is lower, and the water does not have the capacity to hold as much extra carbon as CO_2. This could ultimately result in the subpolar Atlantic becoming a source for anthropogenic CO_2 rather than a sink, as it may not have the capacity to hold the extra CO_2 being passed to it from the south.

BGD
11, 14551–14585, 2014

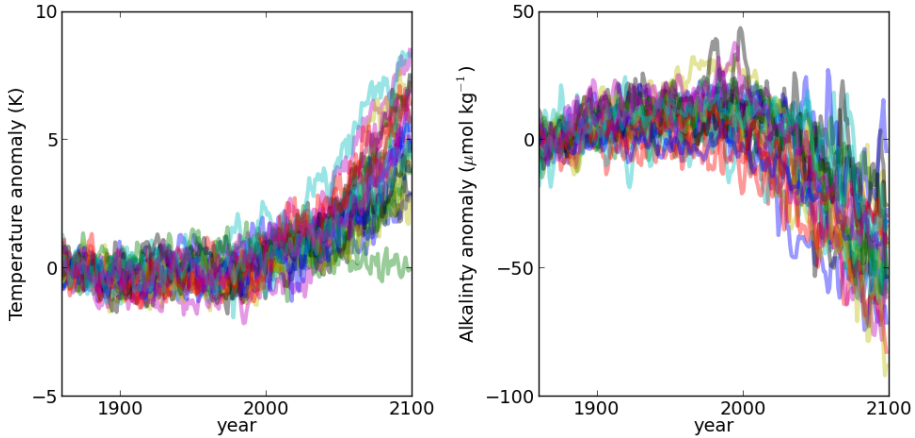

Figure 10. Subpolar North Atlantic surface ocean temperature and alkalinity plotted from the ESPPE simulations as anomalies from their respective first 20 year mean values.

BGD
11, 14551–14585, 2014

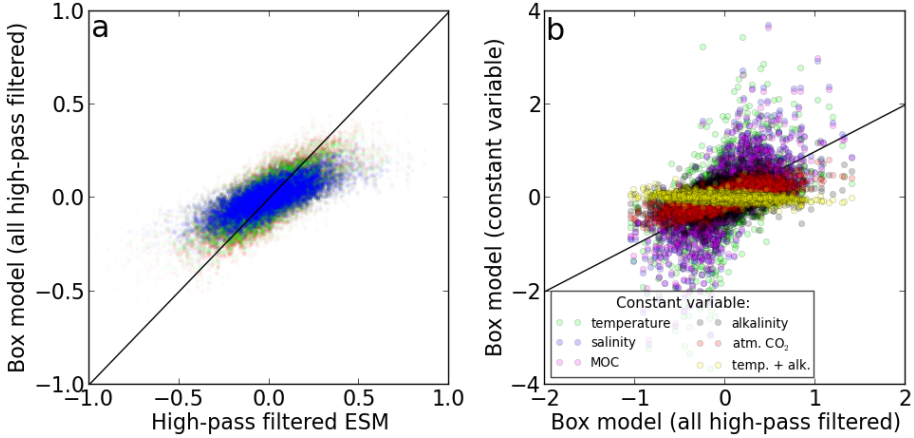

Figure 11. (a) High-pass filtered ESPPE subpolar Atlantic air–sea CO_2 flux plotted against box model estimates of that same flux using the top three box model parameter sets (Table 2) in red, green and blue respectively, but forced with high-pass filtered input time-series. **(b)** All box model inputs (high-pass filtered) plotted against all box model inputs (high-pass filtered) but one variable at a time held constant. The constant variable in each case is named within the legend.

BGD
11, 14551–14585, 2014